

doi:

T.M. PINCHUK-RUGAL,¹ O.P. DMYTRENKO,¹ M.P. KULISH,¹ L.A. BULAVIN,¹
O.S. NYCHYPORENKO,¹ YU.E. GRABOVSKYI,¹ M.A. ZABOLOTNYI,¹
V.V. STRELCHUK,² A.S. NIKOLENKO,² V.V. SHLAPATSKA,³ V.M. TKACH⁴

¹Taras Shevchenko National University of Kyiv

(2, Prosp. Academician Glushkov, Kyiv 03022, Ukraine)

²V.E. Lashkaryov Institute of Semiconductor Physics, Nat. Acad. of Sci. of Ukraine

(41, Prosp. Nauky, Kyiv 03028, Ukraine)

³L.V. Pysarzhevskiy Institute of Physical Chemistry, Nat. Acad. of Sci. of Ukraine

(31, Nauka Ave., Kyiv 03028, Ukraine)

⁴V.N. Bakul Institute for Superhard Materials, Nat. Acad. of Sci. of Ukraine

(2, Autozavodska Str., Kyiv 04074, Ukraine)

RADIATION-INDUCED DAMAGES IN MULTI-WALLED CARBON NANOTUBES AT ELECTRON IRRADIATION

PACS 61.48.De, 61.80.Fe

The morphology, X-ray diffraction patterns, and Raman scattering spectra of multi-walled carbon nanotubes (MWCNTs) synthesized by the methods of chemical vapor deposition and low-temperature catalytic conversion of carbon monoxide in the presence of hydrogen have been studied. Depending on the method of nanotube synthesis, a substantial difference of the correlation between their separate layers took place. In the case of MWCNT irradiation with high-energy electrons with the energy $E_e = 1.8$ MeV to various absorption doses, changes in the structure and the ratio of integral intensities of D- and G-bands in the Raman spectra were observed, which testifies to the enhancement of the interlayer correlation owing to the formation of sp^3 -hybridized bonds between nanotube layers at radiation-induced damages.

Keywords: multiwalled carbon nanotubes, X-ray diffraction, Raman scattering, electron irradiation, radiation-induced damages, destruction.

1. Introduction

Carbon nanotubes are characterized by unique mechanical, thermal, conducting, optical, emission, and sorption properties, which are responsible for their wide application in various branches [1–9]. In view of their important properties and a considerable length-to-diameter geometrical ratio (about 1000), nanotubes are used as filling agents in polymer composites. The influence of ordinary macroscopic fillers manifests itself at a content of 10–30 wt.%, at which a lot of important advantages of polymers can be lost. However, if nanotubes are inserted into a polymer matrix, the composite properties consider-

ably change already at a nanotube content of 0.1–1.0 wt.%. In the latter case, there is no negative influence of filling agents on the functional characteristics of polymers, which is especially required at their application as constructional materials [10–13]. At the same time, the properties of nanotubes substantially depend on the method of their manufacture, which is associated with their defect state.

In this work, the influence of the ionizing irradiation with high-energy electrons to low absorption doses ranging from 0 to 4.0 MGy on the structure and vibrational properties of multi-walled carbon nanotubes (MWCNTs) synthesized by various methods has been studied.

2. Experimental Technique

In this work, MWCNTs synthesized with the use of the chemical vapor deposition (CVD) method (NanocylTM, Sambreville, Belgium) are studied. The nanotube diameter d was equal to 9.5 nm, and the

© T.M. PINCHUK-RUGAL, O.P. DMYTRENKO,
M.P. KULISH, L.A. BULAVIN,
O.S. NYCHYPORENKO, YU.E. GRABOVSKYI,
M.A. ZABOLOTNYI, V.V. STRELCHUK,
A.S. NIKOLENKO, V.V. SHLAPATSKA,
V.M. TKACH, 2015

length L to $1.3 \mu\text{m}$. In addition, we also study MWCNTs obtained by the method of low-temperature catalytic conversion (LTCC) of carbon monoxide in the presence of hydrogen. In this case, iron oxides were used as synthesis catalysts. The reaction of carbon production occurred at temperatures $490\text{--}560 \text{ }^\circ\text{C}$.

The MWCNT morphology was studied with the help of a scanning electron microscope (SEM) Zeiss EVO 60. The electron beam was created using a tungsten cathode and a system of electron acceleration (from 0.1 to 40 keV).

The crystal structure was analyzed in the framework of the X-ray diffraction method, by using $\text{CoK}\alpha$ radiation ($\lambda = 0.17902 \text{ nm}$). The measurements were carried out using the Bragg–Brentano focusing geometry. The registration was fulfilled in the discrete regime in the angular interval from 10 to 90° with a step of 0.1° .

The Raman spectra were studied with the help of a triple spectrometer Horiba Jobin Yvon T64000, a spectrometer DFS-24, and lasers Ar + LGN-404 and LGN-503 with $\lambda_{\text{exc}} = 514.5 \text{ nm}$. The Raman spectra were registered at a power of 2 W/cm^2 .

Specimens were irradiated with electrons emitted from a linear electron accelerator ILU-6. The electron energy amounted to $E_6 = 1.8 \text{ MeV}$. Absorption doses were selected to equal $1.0\text{--}4.0 \text{ MGy}$. The specimen temperature during irradiation did not exceed 333 K .

3. Results and Their Discussion

Depending on the method used to fabricate MWCNTs, a complicated defect structure is formed in them, which assumes the existence of free radicals owing to the break of C–C bonds as a result of the appearance of vacancies, complexes of vacancies, and diamond- and graphite-like structures with various ratios between the sp^3 - and sp^2 -hybridized states. The presence of a definite set of various structural defects evidently affects the degree of interlayer correlations, microstresses, and crystallite dimensions. One may expect that, under the action of ionizing radiation and owing to the radiation-induced defect formation, the parameters of MWCNTs will change both toward their improvement due to the interlayer linkage and toward the worsening of layer packing stabilization as a result of the interstitial cluster formation and the nanotube amorphization.

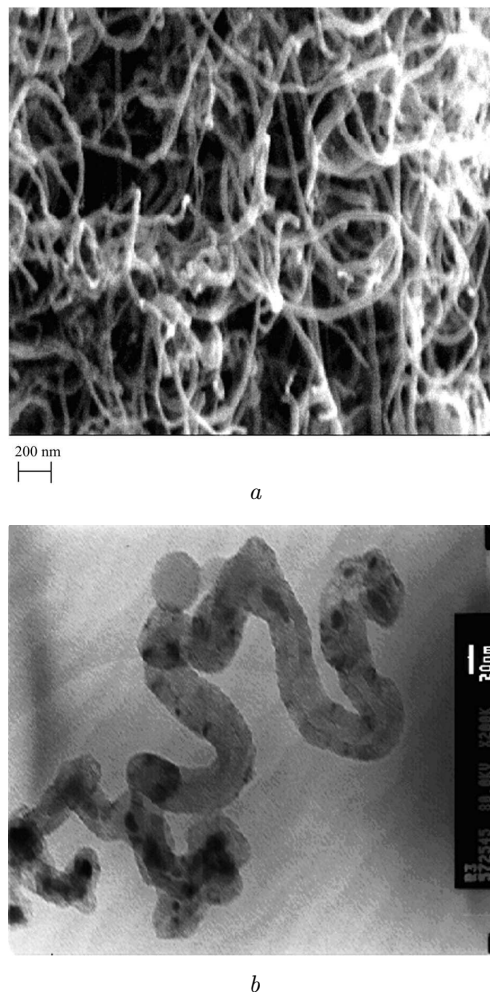


Fig. 1. SEM images of MWCNTs synthesized with the use of the chemical vapor deposition (*a*) and low-temperature catalytic conversion (*b*) methods

In Fig. 1, SEM images of MWCNTs obtained using the CVD and LTCC methods are shown. One can see that the MWCNTs synthesized by the CVD method are in the bundle state (Fig. 1, *a*), which is a result of the van der Waals interaction between separate nanotubes. The external diameter of MWCNTs equals $60\text{--}80 \text{ nm}$, and their length is $1.0 \mu\text{m}$. Carbon nanotubes obtained by the LTCC method have similar parameters, but they are not entangled (Fig. 1, *b*).

In Fig. 2, *a*, the X-ray diffraction patterns for powders of MWCNTs synthesized by the CVD method obtained before the electron irradiation to various low absorption doses and after it are depicted. Figure 2, *b*

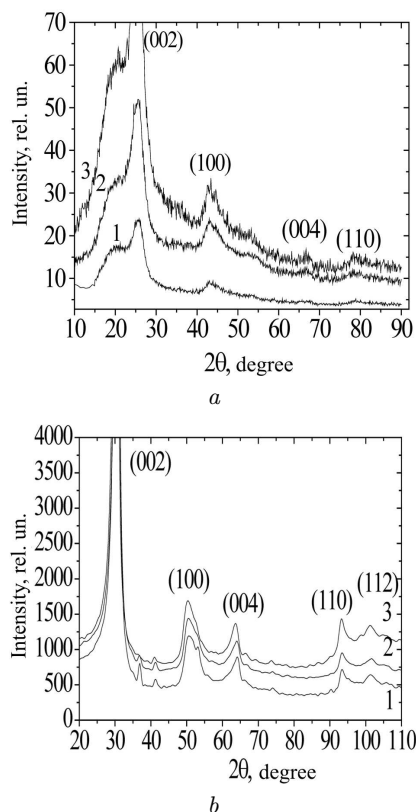


Fig. 2. X-ray diffraction patterns for MWCNTs synthesized by the chemical vapor deposition (a) and low-temperature catalytic conversion (b) methods. Panel a: before irradiation (1) and after electron irradiation to absorption doses of 1.0 (2) and 2.0 MGy (3). Panel b: before irradiation (1) and after electron irradiation to absorption doses of 3.0 (2) and 4.0 MGy (3). $E_e = 1.8$ MeV and $\lambda_{\text{CoK}\alpha} = 0.1790$ nm

demonstrates the X-ray diffraction patterns for powders of MWCNTs synthesized by the LTCC method registered at high absorption doses.

The experimental results testify that the nanotubes produced by the CVD method (Fig. 2, a) have a hexagonal structure with the pronounced reflection (002), which corresponds to the packing of various graphene layers in MWCNTs in the direction c , i.e. perpendicularly to the tube axis [14]. One can see that the intensities of reflections (004) and (110) are weak, and peak (112) is absent. Those facts testify to an insignificant interlayer correlation, i.e. to the absence of ordering in the arrangement of layers for this type of nanotubes. After the high-energy electron irradiation to low absorption doses, the pattern changes weakly.

1152

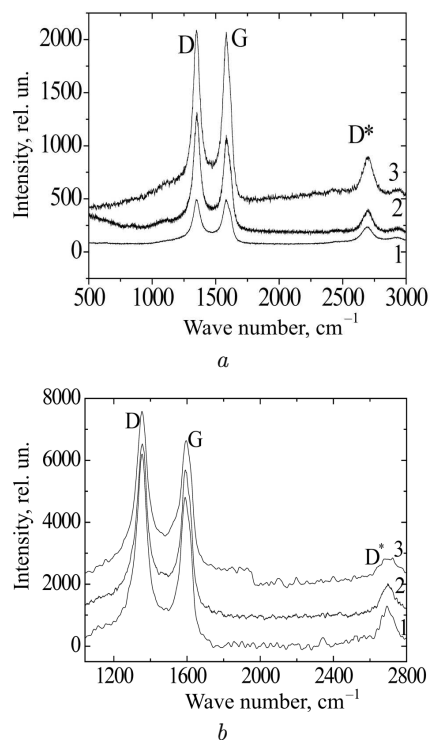


Fig. 3. Raman spectra for MWCNTs synthesized by the chemical vapor deposition (a) and low-temperature catalytic conversion (b) methods. Panel a: before irradiation (1) and after electron irradiation to absorption doses of 1.0 (2) and 2.0 MGy (3). Panel b: before irradiation (1) and after electron irradiation to absorption doses of 3.0 (2) and 4.0 MGy (3). $\lambda_{\text{exc}} = 514.5$ nm and $E_e = 1.8$ MeV

For carbon nanotubes obtained using the LTCC method (Fig. 2, b), the growth of the interlayer correlation, which manifests itself in an increase in the diffraction reflection (112) intensity, points to the stabilizing role of interstitial atoms, owing to which the van der Waals interaction in nanotubes is locally strengthened by bonds inherent to diamond crystals. Attention is attracted by the fact that reflection (100) is appreciably asymmetric, because it is characterized by a stronger intensity growth from its small-angle side and a broadening. A modulation of the intensity within the Bragg reflection limits takes place. Such a non-uniform distribution of the intensity testifies that the interlayer packing is influenced by the in-plane correlations between atoms in the graphene networks, which was also observed for disordered graphite with interlayer correlations [15].

Changes in the local structure of MWCNTs owing to their radiation-induced modifications also affect the Raman spectra of nanotubes in the interval of main vibrational modes D, G, and D*.

It is worth noting that, in the Raman spectra for MWCNTs, active are those fundamental vibrational modes that correspond to radial breathing vibrations, the bands of which are located in the low-frequency interval, as well as to valence vibrations, the G-band of which is in a vicinity of 1585 cm^{-1} . Valence vibrations, owing to the coexistence of nanotubes with different chiralities, undergo splitting. Since achiral nanotubes with the armchair and zigzag symmetries are the most stable, the band of valence vibrations is a doublet, as a rule. At the same time, this band can also become complicated, because, besides the chiral splitting, an additional one arises within the limits of this band, which is associated with the existence of nanotubes characterized by different diameters. Hence, each component of the chiral doublet has a fine structure, the form of which is determined by a set of nanotubes with various diameters. In this case, the splitting of chiral and fine structure components increases, as the diameter of nanotubes diminishes.

In Fig. 3, the Raman spectra of MWCNTs obtained by the CVD and LTCC methods are exhibited in the frequency interval of D- and G-bands. One can see that, for MWCNTs obtained by the CVD method, the intensity of band D is comparable with that of band G. This fact testifies to a substantial role of the disordering in the MWCNT structure. As the distortions decrease and the nanotube diameter grows, the G-band shifts to the position of the graphite E_{2g} mode (1585 cm^{-1}). In this case, the intensity of D-band decreases (it is absent for the ordered graphite). Hence, as the external diameter of MWCNT grows, the MWCNT structure tends to that of graphite. The interlayer correlation grows at that as a consequence of a reduction in the displacement of hexagonal layers, which reveals itself more strongly in nanotubes with a small diameter.

For the carbon nanotubes obtained by the LTCC method, when the absorption dose grows to 3.0 and, especially, 4.0 MGy, the decrease of the total intensity of both D- and G-bands is observed, but except near the G-band frequency of 1533 cm^{-1} , where it grows. In the case of 3.0-MGy absorption dose, the ratio between the integrated intensities I_D/I_G is about 1.1, i.e. the formation of diamond-like struc-

tures continues, as it occurred at an absorption dose of 2.0 MGy. The growth of the D-band intensity testifies to larger destructions in the nanotube structure at higher fluences. At an absorption dose of 4.0 MGy, degradation effects increase, which is testified by the intensity growth of the D-band ($I_D/I_G = 1.2$) and the increase of the low-frequency shoulder of the G-band.

Hence, the processes of interlayer linkage for carbon nanotubes manifest themselves more strongly at low absorption doses of 1.0–3.0 MGy.

4. Conclusions

Radiation-induced damages of multi-walled carbon nanotubes (MWCNTs) by the high-energy electron irradiation ($E_e = 1.8\text{ MeV}$) substantially depend on the conditions of synthesis and the absorption dose. At low absorption doses within the interval from 1.0 to 4.0 MGy, the interlayer linkage prevails as a consequence of the formation of diamond-like sp^3 -hybridized bonds. It is accompanied by the growth of both the intensity of the diffraction reflection (112) and the asymmetry of peak (110), which are associated with the interlayer correlation between the atomic arrangements in separate layers of nanotubes.

The processes of nanotube degradation manifest themselves not only as a reduction of the intensities of D- and G-bands, but also as a growth of the ratio between the integrated intensities I_D/I_G .

1. A.V. Yeletskii, Usp. Fiz. Nauk **167**, 945 (1997).
2. A.V. Yeletskii, Usp. Fiz. Nauk **172**, 401 (2002).
3. A.V. Yeletskii, Usp. Fiz. Nauk **174**, 1191 (2004).
4. A.V. Yeletskii, Usp. Fiz. Nauk **179**, 225 (2009).
5. A.V. Yeletskii, Usp. Fiz. Nauk **180**, 897 (2010).
6. E.G. Rakov, Zh. Neorg. Khim. **44**, 1827 (1999).
7. E.G. Rakov, Usp. Khim. **69**, 41 (2000).
8. E.G. Rakov, Usp. Khim. **70**, 934 (2001).
9. A.I. Vorobyova, Usp. Fiz. Nauk **180**, 265 (2010).
10. B.E. Kibrade and J.N. Coleman, J. Appl. Phys. **92**, 4024 (2002).
11. P.J. Harris, Int. Mater. Rev. **49**, 31 (2004).
12. M. Baibaras and P. Gomes-Romero, J. Nanosci. Nanotechn. **6**, 14 (2006).
13. S.-Y. Fu, Z.-K. Chen, S. Hong, and C.C. Han, Carbon **47**, 3192 (2009).
14. D. Reznik and C.H. Neumann, Phys. Rev. B **52**, 116 (1995).
15. F. Benueu, C. l'Huillier, and J.-P. Salvetat, Phys. Rev. B **59**, 5945 (1999).

Received 09.09.15.

Translated from Ukrainian by O.I. Voitenko

*Т.М. Пінчук-Ругаль, О.П. Дмитренко,
М.П. Куліш, Л.А. Булавін, О.С. Ничипоренко,
Ю.Є. Грабовський, М.А. Заболотний, В.В. Стрельчук,
А.С. Ніколенко, В.В. Шлапацька, В.М. Ткач*

РАДІАЦІЙНІ ПОШКОДЖЕННЯ
БАГАТОСТІННИХ ВУГЛЕЦЕВИХ НАНОТРУБОК
ПРИ ОПРОМІНЕННІ ЕЛЕКТРОНАМИ

Резюме

Досліджено морфологію, рентгенівську дифракцію та комбінаційне розсіяння світла (КРС) багатостінних вуглецевих

нанотрубок (БВНТ), синтезованих методами хімічного осадження (CVD) і низькотемпературної каталітичної конверсії монооксиду вуглецю в присутності водню.

Залежно від методів синтезу нанотрубок має місце суттєва відмінність в кореляції між їх окремими шарами. У випадку опромінення БВНТ високоенергетичними електронами з енергією $E_e = 1,8$ МеВ з різними дозами поглинання спостерігається зміна будови і співвідношення інтегральних інтенсивностей D і G-смуг КРС, що свідчить про покращення міжшарової кореляції за рахунок утворення при радіаційних пошкодженнях sp^3 -гібридизованого зв'язку між шарами нанотрубок.